Electronic Research Archive

https://www.aimspress.com/journal/era

ERA, 34(7): 4486–4511.
DOI: 10.3934/era.2026198
Received: 14 January 2026
Revised: 14 May 2026
Accepted: 18 May 2026
Published: 26 May 2026

Research article

Analysis of a stochastic predator-prey model based on the Ornstein-Uhlenbeck process with Holling-II and Beddington–DeAngelis functional responses

Wenyu Zhang and Xiaohui Ai*

School of Science, Northeast Forestry University, Harbin 150040, China

* **Correspondence:** Email: axh_826@163.com; Tel: +8618345173579.

Abstract: In this paper, we investigated a predator–prey model driven by an Ornstein–Uhlenbeck process and featuring Holling-II and Beddington–DeAngelis functional responses. To begin, the biological significance of the Ornstein-Uhlenbeck process in ecological modeling was illustrated, along with its validity in characterizing random environmental fluctuations. Subsequently, the existence and uniqueness of the global solution for this model were strictly proven and its ultimate boundedness was analyzed. By constructing Lyapunov functions and applying Itô's formula, the existence of the stationary distribution of the system was demonstrated, while sufficient conditions for population extinction were provided. Finally, numerical simulations were conducted to confirm the validity of the conclusions. This work provides a theoretical framework for understanding complex mutualistic-predatory communities under persistent environmental fluctuations.

Keywords: Ornstein-Uhlenbeck process; Holling-II functional response; Beddington–DeAngelis functional response; stationary distribution; extinction

1. Introduction

Studying predator-prey models is a key mathematical approach for analyzing species interactions within ecosystems. Early theoretical research primarily focused on single interspecies relationships, such as pure predation and competition. However, in nature, multiple interactions often coexist among different populations, forming complex networks and giving rise to rich dynamic behaviors [1–3]. The plant-pollinator-herbivore system is a typical example of this complexity. Within this system, herbivores consume plants, pollinators provide pollination services to plants, and plants offer resources like nectar to pollinators. Consequently, this system simultaneously incorporates both mutualistic and predatory interactions, making it an ideal model for exploring the dynamics of complex interspecies interactions.

The mutualistic relationship between plants and pollinators is a crucial component in maintaining ecosystem function. However, increasing evidence indicates that pollinator populations are facing a decline crisis, and their disappearance would lead to the loss of plant diversity and trigger a series of ecological chain reactions [4]. Therefore, studying the dynamic interactions within plant-pollinator-herbivore systems is crucial for understanding and maintaining the stability of agricultural ecosystems. Numerous scholars have conducted theoretical explorations in this field. Yacine et al. [5] revealed mechanisms enabling stable coexistence among the three populations in this system, demonstrating that predation between plants and herbivores suppresses unlimited population growth driven by strong mutualism, thereby promoting system stability. Subsequent studies further examined the impacts of factors, such as human disturbances, phenological synchrony, and spatial heterogeneity [6, 7]. Additionally, research from an adaptive evolutionary perspective has also made progress [8, 9].

It is noteworthy that most of the above studies employed a simplistic additive model when characterizing the effects of pollinators and herbivores on plants, assuming that the two interactions operate independently [10–12]. However, growing experimental evidence indicates that herbivore feeding can induce chemical or morphological changes in plants, thereby reducing their attractiveness to pollinators and indirectly weakening mutualistic strength [13–15]. This regulation of interaction strength by a third species is termed higher-order interactions [16]. For example, Liu et al. [17] studied stochastic logistic models with Lévy noise and derived necessary and sufficient conditions for species persistence and extinction, highlighting the combined effects of stochastic disturbances and interspecific interactions. Molla et al. [18] explored a predator-prey model with Allee effect and nonlinear prey refuge, revealing that indirect interactions between species can significantly alter system stability. Synergistic effects between higher-order interactions and fundamental interspecies relationships are widespread and of considerable magnitude, serving as a key driver of complex dynamical behavior within ecosystems [19]. Incorporating them into ecological theoretical frameworks enhances the realism of population dynamics modeling and enriches existing theoretical research [20–25]. The coupled effects of higher-order interactions, environmental random disturbances, and interspecific fundamental relationships within ecosystems remain poorly understood. Neglecting such coupling readily leads to biased model predictions. Therefore, investigating the effects of higher-order interactions in systems simultaneously involving predation and mutualism is particularly essential. For instance, in predator-prey systems, higher-order interactions mediated by fear effects [26] have been shown to drastically alter system stability, highlighting the necessity of their inclusion in multi-species models.

To capture these complex interactions in the model, the choice of functional response functions is crucial. For predator-prey relationships between plants and herbivores, the classic Holling type II functional response is widely adopted, effectively capturing the saturation effect of predation rates [27, 28]. Conversely, the Beddington-DeAngelis (BD) functional response proves more suitable for mutualistic plant-pollinator interactions and the disturbances herbivores impose on pollinators. By incorporating disturbance terms, it overcomes the limitations of traditional models and improves model fit. First proposed by Beddington and DeAngelis in 1975, this function was originally designed to describe how interference among individual predators affects predation efficiency [29, 30]. Its advantage lies in avoiding the "abundance paradox" found in classical models and more accurately capturing changes in mutualistic or predation intensity when interference agents are present [31]. Recent studies confirm that models incorporating BD-type functional responses better align with observed population dynamics [32–34].

Based on these theories, we construct the following deterministic plant-pollinator-herbivore model:

$$\begin{cases} \frac{dF}{dt} = rF\left(1-\frac{F}{K}\right) + \frac{a_1FP}{1+\alpha F+\beta P+\gamma H} - \frac{a_2FH}{c+F}, \\ \frac{dP}{dt} = \frac{\alpha_1FP}{1+\alpha F+\beta P+\gamma H} - d_1P, \\ \frac{dH}{dt} = \frac{\alpha_2FH}{c+F} - d_2H. \end{cases} \tag{1.1}$$

This model inherits the core structure of the system of ordinary differential equations analyzed in detail by Song [35]. Its key dynamical results provide an important benchmark for our subsequent stochastic generalization. Song's research has rigorously proven the system's forward invariance and dissipativity, equilibrium stability, bifurcation dynamics, and extinction and survival states of this system, which we use as a deterministic benchmark for the stochastic generalization. In this system, $F(t)$, $P(t)$, and $H(t)$ represent the population densities of plants, pollinators, and herbivores at time t, respectively. The parameter r denotes the intrinsic growth rate of plants, while K represents the environmental carrying capacity. The herbivore's predation on plants is described by the Holling type II functional response $\frac{a_2FH}{c+F}$, where a_2 is the maximum feeding rate and c is the saturation constant. The mutualistic interaction between plants and pollinators is modeled by the BD functional response $\frac{a_1FP}{1+\alpha F+\beta P+\gamma H}$, where a_1 is the maximum mutualistic rate and α and β measure the effects of plant and pollinator self-density on mutualistic efficiency, respectively. Crucially, the parameter γ quantifies the suppression intensity of herbivores as disturbers on pollinator visitation efficiency, directly reflecting higher-order interactions. The denominator $1+\alpha F+\beta P+\gamma H$ comprehensively captures the multi-factor constraints on pollinator foraging and pollination efficiency, including the time cost of pollinators handling plants, the intraspecific competition among pollinators, and the interference from herbivores. A positive sign is assigned to this term because pollinators accomplish pollination during foraging on plants, and this mutualistic behavior directly promotes plant reproduction and population growth, thus contributing positively to the plant population dynamics. Parameters α_1 and α_2 represent the conversion efficiencies for the respective interactions. d_1 and d_2 denote the natural mortality rates for pollinators and herbivores, respectively. All parameters in the model are positive, except for r, which can be either positive or negative.

Real ecosystems inevitably experience random fluctuations in their environment. As May [36] pointed out, environmental noise can continuously affect key parameters of population systems, such as intrinsic growth rates and mortality rates. To characterize such persistent environmental disturbances, a common approach is to model parameters as linearly perturbed by Gaussian white noise [37]. For instance, consider the formulations $r(t) = \bar{r} + \frac{\eta_1 dB_1(t)}{dt}$ and $d_1(t) = \bar{d}_1 + \frac{\eta_2 dB_2(t)}{dt}$ where $\bar{r}, \bar{d}_1$ denote long-term means, $B_i(t)$ represents independent standard Brownian motion, and η_i denotes noise intensity. However, this approach suffers from biological shortcomings. Consider the time-averaged value of the parameter over the interval $[0, t]$: $\langle r(t)\rangle := \frac{1}{t}\int_0^t r(s)ds$. Its distribution is

$$\langle r(t)\rangle \sim \mathbb{N}\left(\bar{r}, \frac{\eta_1^2}{t}\right).$$

As $t \to 0^+$, the variance $\frac{\eta_1^2}{t}$ approaches infinity, indicating that the parameter undergoes extreme fluctuations within an extremely short time interval. This behavior is inconsistent with the continuous and gradual disturbance characteristics of environmental noise.

Therefore, we employ the mean-reverting Ornstein-Uhlenbeck (OU) process to simulate the random disturbance of key parameters by environmental noise [38], enabling more precise capture of the impact of parameter heterogeneity on the system [39–41]. To prevent negative values in the mortality parameter, we assume that the logarithm of the mortality parameter is driven by the OU process. Specifically, let $g_1(t) = r(t)$, $g_2(t) = \ln d_1(t)$, and $g_3(t) = \ln d_2(t)$, which satisfy the following stochastic differential equations:

$$dg_i(t) = \beta_i[\bar{g}_i - g_i(t)]dt + \sigma_i dB_i(t), \quad i = 1, 2, 3,$$

where $\bar{g}_i$ denotes the long-term mean level of the parameter, $\beta_i > 0$ represents the regression rate, $\sigma_i > 0$ indicates the volatility intensity, and $B_i(t)$ is an independent standard Brownian motion defined on the complete probability space $(\Omega, \mathcal{F}, \{\mathcal{F}_t\}_{t\geq 0}, \mathbb{P})$, where Ω is the sample space, $\mathcal{F}$ is the filtration, and $\mathcal{F}_t$ denotes the filtration at time t for all $t \geq 0$. According to Mao [42], this equation has a unique solution

$$g_i(t) = \bar{g}_i + [g_i(0) - \bar{g}_i]e^{-\beta_i t} + \sigma_i \int_0^t e^{-\beta_i(t-s)} dB_i(s),$$

Moreover, $g_i(t)$ follows a normal distribution

$$g_i(t) \sim \mathbb{N}\left(\bar{g}_i + [g_i(0) - \bar{g}_i]e^{-\beta_i t}, \frac{\sigma_i^2}{2\beta_i}\left(1 - e^{-2\beta_i t}\right)\right).$$

Its expectation and variance satisfy

$$\lim_{t\to 0^+} \mathbb{E}[g_i(t)] = g_i(0), \quad \lim_{t\to 0^+} \mathrm{Var}[g_i(t)] = 0; \quad \lim_{t\to\infty} \mathbb{E}[g_i(t)] = \bar{g}_i, \quad \lim_{t\to\infty} \mathrm{Var}[g_i(t)] = \frac{\sigma_i^2}{2\beta_i}.$$

This indicates that parameter fluctuations are confined within a finite range, better aligning with the continuous disturbance characteristics of environmental noise.

Based on the above analysis, we randomize the deterministic model to obtain the following system of stochastic differential equations driven by an OU process:

$$\begin{cases} dF(t) = F(t)\left[g_1(t)\left(1 - \frac{F(t)}{K}\right) + \frac{a_1 P(t)}{1+\alpha F(t)+\beta P(t)+\gamma H(t)} - \frac{a_2 H(t)}{c+F(t)}\right]dt, \\ dP(t) = P(t)\left[\frac{\alpha_1 F(t)}{1+\alpha F(t)+\beta P(t)+\gamma H(t)} - e^{g_2(t)}\right]dt, \\ dH(t) = H(t)\left[\frac{\alpha_2 F(t)}{c+F(t)} - e^{g_3(t)}\right]dt, \\ dg_1(t) = \beta_1\left[\overline{g}_1 - g_1(t)\right]dt + \sigma_1 dB_1(t), \\ dg_2(t) = \beta_2\left[\overline{g}_2 - g_2(t)\right]dt + \sigma_2 dB_2(t), \\ dg_3(t) = \beta_3\left[\overline{g}_3 - g_3(t)\right]dt + \sigma_3 dB_3(t). \end{cases} \tag{1.2}$$

In this stochastic system, $g_1(t)$ directly represents the plant's intrinsic growth rate, while $e^{g_2(t)}$ and $e^{g_3(t)}$ denote the pollinator and herbivore natural mortality rates, respectively, ensuring that mortality rates remain positive.

Existing studies have predominantly examined higher-order interactions or simple random perturbations in isolation, while research coupling both with interspecific mutualistic-predatory relationships remains scarce. This model fills the gap by combining higher-order interactions, mean-reverting OU noise, and composite functional responses, offering insights for pollinator conservation under realistic

environmental variability. This model represents a continuation and extension of ecological stochastic modeling. In this paper, we aims to systematically investigate the dynamical properties of such stochastic models. Subsequently, in Section 3, we prove the existence of a unique global solution for system (1.2) and verify its ultimate boundedness, the existence of stationary distributions, and extinction conditions. Finally, in Section 4, numerical simulations are performed to verify the theoretical results and demonstrate the validity of these findings. We aims to provide theoretical insights for understanding complex community dynamics involving mutualism, predation, and higher-order interactions under stochastic conditions, thereby offering quantitative references for practical applications such as pollinator conservation and agricultural ecosystem regulation.

2. Preliminaries

To simplify the proof, we define two necessary sets: $\mathbb{G}_n = (-n, n) \times (-n, n) \times (-n, n)$ and $\mathbb{R}^n_+ = \{(x_1, \cdots, x_n) \in \mathbb{R}^n \mid x_k > 0, 0 \le k \le n\}$, where $\|\cdot\|$ represents the Euclidean norm. Consider a stochastic differential equation of the following form:

$$dX(t) = \xi(t, X(t))dt + \sum_{j=1}^{n} \varsigma_j(t, X(t))dB_j(t). \tag{2.1}$$

Using Khasminskii's lemma [43], it can be proven that system (1.2) possesses a stationary solution for any initial value under random conditions.

Lemma 2.1. *(Khasminskii) Assume that the vectors $\xi(s, x)$, $\varsigma_1(s, x), \ldots, \varsigma_l(s, x)$ (where $s \in [t_0, T]$, $x \in \mathbb{R}^m$) are continuous functions of the variables (s, x) and that there exists a constant M such that the relevant conditions hold throughout the entire domain*

$$|\xi(s, x) - \xi(s, y)| + \sum_{j=1}^{l} |\varsigma_j(s, x) - \varsigma_j(s, y)| \le M|x - y|,$$

$$|\xi(s, x)| + \sum_{j=1}^{l} |\varsigma_j(s, x)| \le M(1 + |x|).$$

Additionally, there exists a non-negative function $V_*(x)$ satisfying the following requirements:

$$\mathcal{L}V_*(x) \le -1, \quad \forall x \in \mathbb{R}^m \setminus \mathbb{H}, \tag{2.3}$$

Among these, if $\mathbb{H}$ is a compact subset of $\mathbb{R}^m$, then the Markov process (2.1) *possesses at least one stationary solution $X(t)$, which corresponds to a stationary distribution $\omega(\cdot)$ in the space $\mathbb{R}^m$.*

Lemma 2.2. *(Strong Law of Large Numbers [44]) Let $M = \{M_t\}_{t\ge 0}$ be a real-valued continuous local martingale with initial value 0 at $t = 0$. Under this assumption, the following conclusion holds almost surely:*

$$\lim_{t\to\infty} \langle M, M\rangle_t = \infty, \quad \lim_{t\to\infty} \frac{M_t}{\langle M, M\rangle_t} = 0, \quad \limsup_{t\to\infty} \frac{\langle M, M\rangle_t}{M_t} < \infty, \quad \lim_{t\to\infty} \frac{M_t}{t} = 0.$$

From a more general perspective, if $S = \{S_t\}_{t\ge 0}$ is a continuous, adapted, and increasing process satisfying $\lim_{t\to\infty} S_t = \infty$ and $\int_0^\infty \frac{d\langle M,M\rangle_t}{(1+S_t)^2} < \infty$, then we can conclude that $\lim_{t\to\infty} \frac{M_t}{S_t} = 0$ a.s.

Lemma 2.3. *(Itô's formula [42]) Let $x(t)$ be an Itô process on $t \geq 0$, with the corresponding stochastic differential given by*

$$dx(t) = f(t)dt + g(t)dB_t,$$

Here, $f \in L^1(\mathbb{R}_+;\mathbb{R})$ and $g \in L^2(\mathbb{R}_+;\mathbb{R})$. Let $V \in C^{2,1}(\mathbb{R}\times\mathbb{R}_+;\mathbb{R})$. Then, $V(x(t),t)$ also belongs to the class of Itô processes, and its corresponding stochastic differential form is

$$dV(x(t),t) = \left[V_t(x(t),t) + V_x(x(t),t)f(t) + \frac{1}{2}V_{xx}(x(t),t)g^2(t)\right]dt + V_x(x(t),t)g(t)dB_t \quad a.s.$$

3. Results

3.1. Existence and uniqueness of the global solution

Theorem 3.1. *For any initial values $(F(0),P(0),H(0),g_i(0)) \in \mathbb{R}^3_+ \times \mathbb{R}^3$ where $i = 1,2,3$, the system (1.2) possesses a unique global solution $(F(t),P(t),H(t),g_i(t)) \in \mathbb{R}^3_+ \times \mathbb{R}^3$ exists for $t \geq 0$, and this solution remains in the space $\mathbb{R}^3_+ \times \mathbb{R}^3$ with probability 1.*

Proof. It can be seen that the coefficients of model (1.2) satisfy the local Lipschitz condition. Therefore, for any given initial values $(F(0),P(0),H(0),g_i(0))$ (where $i = 1,2,3$), the system (1.2) has a unique local solution $(F(t),P(t),H(t),g_i(t))$ on the interval $[0,\tau_e)$, where τ_e denotes the explosion time [42]. To prove that this solution is global, it suffices to show that $\tau_e = \infty$.

Choose a sufficiently large n such that each component of $\ln F(0)$, $\ln P(0)$, $\ln H(0)$, and $g_i(0)$ $(i = 1,2,3)$ lies within the interval $[-n,n]$. Denote this n as n_0. For all n belonging to the set of integers satisfying $n \geq n_0$, we define the stopping time τ_n as follows:

$$\tau_n = \inf\{t \in [0,\tau_e] \mid \ln F(t) \notin (-n,n) \text{ or } \ln P(t) \notin (-n,n) \text{ or } \ln H(t) \notin (-n,n) \text{ or } g_i(t) \notin (-n,n)\},$$

Here, $i = 1,2,3$. As n increases, τ_n also increases. Let $\tau_\infty = \lim_{n\to\infty}\tau_n$, then $\tau_\infty \leq \tau_e$. Therefore, it suffices to show that $\tau_\infty = \infty$ holds almost surely. Suppose this assertion does not hold. Then, there exist constants $T > 0$ and $\varepsilon \in (0,1)$ such that there is an integer $n_1 \geq n_0$ satisfying the following conditions:

$$\mathbb{P}\{\tau_n \leq T\} \geq \varepsilon, \quad \forall n \geq n_1. \tag{3.1}$$

For any $t \leq \tau_n$, we define a nonnegative Lyapunov function $V(F(t),P(t),H(t),g_i(t))$ mapping from $\mathbb{R}^3_+ \times \mathbb{R}^3$ to $\mathbb{R}$ as follows:

$$V(F,P,H,g_i) = F - 1 - \ln F + P - 1 - \ln P + H - 1 - \ln H + \frac{g_1^4}{4} + \frac{g_2^4}{4} + \frac{g_3^4}{4}. \tag{3.2}$$

Based on Itô's formula, we can derive that

$$dV = \mathcal{L}Vdt + \sigma_1 g_1^3 dB_1(t) + \sigma_2 g_2^3 dB_2(t) + \sigma_3 g_3^3 dB_3(t), \tag{3.3}$$

where

$$\mathcal{L}V = (F-1)\left[g_1\left(1-\frac{F}{K}\right) + \frac{a_1P}{1+\alpha F+\beta P+\gamma H} - \frac{a_2H}{c+F}\right] + (P-1)\left[\frac{\alpha_1 F}{1+\alpha F+\beta P+\gamma H} - e^{g_2}\right]$$
$$+ (H-1)\left[\frac{\alpha_2 F}{c+F} - e^{g_3}\right] + \sum_{i=1}^{3}\left(\frac{3}{2}g_i^2\sigma_i^2 + g_i^3\beta_i(\overline{g_i} - g_i)\right)$$

Through calculations, the following results can be obtained:

$$\begin{aligned}\mathcal{L}V \leq & \left(|g_1| + \frac{g_1}{K} + \frac{a_1+\alpha_1}{\beta}\right)F - \frac{|g_1|}{K}F^2 + \left(\frac{a_2}{c} + \alpha_2 - e^{g_3}\right)H \\ & + |g_1| + e^{g_2} + e^{g_3} + \sum_{i=1}^{3}\left(\frac{3}{2}g_i^2\sigma_i^2 + \beta_i\overline{g}_i g_i^3 - \beta_i g_i^4\right) \\ & \leq \Pi_0 < \infty\end{aligned}$$

where

$$\begin{aligned}\Pi_0 = \sup_{(F,P,H,g_i)\in\mathbb{R}_+^3\times\mathbb{R}^3} & \left\{\left(|g_1| + \frac{g_1}{K} + \frac{a_1+\alpha_1}{\beta}\right)F - \frac{|g_1|}{K}F^2 + \left(\frac{a_2}{c} + \alpha_2 - e^{g_3}\right)H \right. \\ & \left. + |g_1| + e^{g_2} + e^{g_3} + \sum_{i=1}^{3}\left(\frac{3}{2}g_i^2\sigma_i^2 + \beta_i\overline{g}_i g_i^3 - \beta_i g_i^4\right)\right\}.\end{aligned}$$

Furthermore,

$$dV \leq \Pi_0 dt + \sigma_1 g_1^3 dB_1(t) + \sigma_2 g_2^3 dB_2(t) + \sigma_3 g_3^3 dB_3(t). \tag{3.4}$$

Integrating inequality (3.4) over the interval from 0 to $\tau_n \wedge T$ yields

$$\int_0^{\tau_n\wedge T} dV \leq \int_0^{\tau_n\wedge T} \Pi_0 dt + \int_0^{\tau_n\wedge T} \left[\sigma_1 g_1^3 dB_1(t) + \sigma_2 g_2^3 dB_2(t) + \sigma_3 g_3^3 dB_3(t)\right]. \tag{3.5}$$

Taking the expectation of both sides of the equation yields

$$\mathbb{E}\left[V\left(F(\tau_n\wedge T), P(\tau_n\wedge T), H(\tau_n\wedge T), g_i(\tau_n\wedge T)\right)\right] \leq V(F(0), P(0), H(0), g_i(0)) + \Pi_0 T. \tag{3.6}$$

For $n \geq n_1$, set $\Omega_n = \{\tau_n \leq T\}$. From Eq (3.1), we have $\mathbb{P}(\Omega_n) \geq \varepsilon$. It should be noted that for every $\omega \in \Omega_n$, there exists a corresponding n such that $\ln F(\tau_n, \omega)$, $\ln P(\tau_n, \omega)$, $\ln H(\tau_n, \omega)$, and $g_i(\tau_n, \omega)$ take the values $-n$ or n. Hence, we obtain

$$\begin{aligned}V(F(0), P(0), H(0), g_i(0)) + \Pi_0 T &\geq \mathbb{E}\left[I_{\Omega_n(\omega)} V\left(F(\tau_n,\omega), P(\tau_n,\omega), H(\tau_n,\omega), g_i(\tau_n,\omega)\right)\right] \\ &\geq \varepsilon \min\left\{e^{-n} - 1 + n, e^n - 1 - n, \frac{n^4}{4}\right\}, \quad i = 1,2,3,\end{aligned}$$

Here, $I_{\Omega_n(\omega)}$ denotes the indicator function of Ω_n. As $n \to \infty$, we obtain

$$\infty > V(F(0), P(0), H(0), g_i(0)) + \Pi_0 T = \infty, \quad i = 1,2,3. \tag{3.7}$$

This result contradicts previous conclusions, thus establishing that $\tau_\infty = \infty$ holds almost certainly. The proof is complete.

□

3.2. Ultimate boundedness

In natural ecosystems, the availability of resources has an upper limit, which constrains the unlimited growth of populations. Over time, population density does not rise indefinitely but instead enters a relatively stable state. Based on this, establishing the theoretical boundedness of system (1.2) is crucial. To achieve this goal, we first introduce the concept of stochastic boundedness [45].

Definition 3.1. [45] For any $\varepsilon \in (0,1)$, if there exists a constant $\varpi = \varpi(\omega)$ such that for any initial values (F_0, P_0, H_0, g_{i0}) (where $i = 1,2,3$) the solutions to system (1.2) possess the following property, then system (1.2) is said to be stochastically ultimately bounded:

$$\limsup_{t\to\infty} \mathbb{P}\left(\sqrt{F^2+P^2+H^2} > \varpi\right) < \varepsilon. \tag{3.8}$$

Lemma 3.1. *For any initial values* $(F(0), P(0), H(0), g_i(0))$ *belonging to* $\mathbb{R}^3_+ \times \mathbb{R}^3$ *(where* $i = 1,2,3$*), the solution to system* (1.2) *possesses the following properties:*

$$\limsup_{t\to\infty} \mathbb{E}\left[|(F,P,H)|^q\right] \le Q(q), \tag{3.9}$$

Here, $q \in (0,1)$ *and* $Q(q)$ *is a constant independent of the initial values* $(F(0), P(0), H(0), g_i(0))$.

Proof. Define a Lyapunov function V_1 mapping from $\mathbb{R}^3_+ \times \mathbb{R}^3$ to $\mathbb{R}$ as follows:

$$V_1 = \frac{F^q(t)}{q} + \frac{P^q(t)}{q} + \frac{H^q(t)}{q} + \sum_{i=1}^{3} \frac{g_i^{2q+2}(t)}{2q+2}.$$

Applying Itô's formula to V_1 yields

$$dV_1 = \mathcal{L}V_1 dt + \sigma_1 g_1^{2q+1} dB_1(t) + \sigma_2 g_2^{2q+1} dB_2(t) + \sigma_3 g_3^{2q+1} dB_3(t),$$

where

$$\begin{aligned}\mathcal{L}V_1 = {} & F^q\left[g_1\left(1-\frac{F}{K}\right) + \frac{a_1 P}{1+\alpha F+\beta P+\gamma H} - \frac{a_2 H}{c+F}\right] + P^q\left[\frac{\alpha_1 F}{1+\alpha F+\beta P+\gamma H} - e^{g_2}\right] \\ & + H^q\left[\frac{\alpha_2 F}{c+F} - e^{g_3}\right] + \sum_{i=1}^{3}\left(\frac{2q+1}{2} g_i^{2q}\sigma_i^2 + \beta_i g_i^{2q+1}(\overline{g_i} - g_i)\right)\end{aligned}$$

Therefore,

$$\begin{aligned}\mathcal{L}V_1 \le {} & \left(|g_1| + \frac{a_1}{\beta}\right) F^q - \frac{|g_1|}{K} F^{q+1} - (e^{g_2} - \frac{\alpha_1}{\alpha}) P^q - (e^{g_3} - \alpha_2) H^q \\ & + \sum_{i=1}^{3}\left(\frac{2q+1}{2} g_i^{2q}\sigma_i^2 + \beta_i \overline{g}_i g_i^{2q+1} - \beta_i g_i^{2q+2}\right)\end{aligned} \tag{3.10}$$

Let $\eta = q\min\{\beta_1, \beta_2, \beta_3\}$. By applying Itô's formula once more, we obtain

$$\begin{aligned} d\left(e^{\eta t} V_1\right) &= \eta e^{\eta t} V_1 dt + e^{\eta t} dV_1 \\ &= e^{\eta t}\left(\eta V_1 + \mathcal{L}V_1\right) dt + e^{\eta t} \sum_{i=1}^{3} \sigma_i g_i^{2q+1} dB_i(t). \end{aligned} \tag{3.11}$$

Integrating both sides of Eq (3.11) over the interval from 0 to t and then taking the expectation of the result yields

$$\mathbb{E}\left(e^{\eta t} V_1\right) = \mathbb{E}\left(V_1(F(0), P(0), H(0), g_i(0))\right) + \int_0^t \mathbb{E}\left(e^{\eta s}(\eta V_1 + \mathcal{L}V_1)\right) ds, \quad i = 1,2,3. \tag{3.12}$$

By analyzing the expression of $\mathcal{L}V_1$, we can conclude that

$$\begin{aligned}\eta V_1 + \mathcal{L}V_1 \leq & \sup_{(F,P,H,g_i)\in\mathbb{R}^3_+\times\mathbb{R}^3}\left\{\frac{\eta F^q}{q}+\frac{\eta P^q}{q}+\frac{\eta H^q}{q}+\sum_{i=1}^{3}\frac{\eta g_i^{2q+2}}{2q+2}+\left(|g_1|+\frac{a_1}{\beta}\right)F^q-\frac{|g_1|}{K}F^{q+1}-(e^{g_2}-\frac{\alpha_1}{\alpha})P^q\right.\\ & \left.-(e^{g_3}-\alpha_2)H^q+\sum_{i=1}^{3}\left(\frac{2q+1}{2}g_i^{2q}\sigma_i^2+\beta_i\overline{g}_i g_i^{2q+1}-\beta_i g_i^{2q+2}\right)\right\}\\ \leq & \sup_{(F,P,H,g_i)\in\mathbb{R}^3_+\times\mathbb{R}^3}\left\{\left(|g_1|+\frac{a_1}{\beta}+\beta_1\right)F^q-\frac{|g_1|}{K}F^{q+1}-(e^{g_2}-\beta_2-\frac{\alpha_1}{\alpha})P^q-(e^{g_3}-\beta_3-\alpha_2)H^q\right.\\ & \left.+\sum_{i=1}^{3}\left((q+1)g_i^{2q}\sigma_i^2+\beta_i\overline{g}_i g_i^{2q+1}-\frac{\beta_i}{2}g_i^{2q+2}\right)\right\}:=\kappa_1(q).\end{aligned} \tag{3.13}$$

Substituting Eq (3.13) into Eq (3.12) yields

$$\mathbb{E}\left(e^{\eta t}V_1\right)\leq\mathbb{E}\left(V_1(F(0),P(0),H(0),g_i(0))\right)+\mathbb{E}\int_0^t e^{\eta s}\kappa_1(q)ds.$$

Then,

$$e^{\eta t}\mathbb{E}V_1\leq\mathbb{E}\left(V_1(F(0),P(0),H(0),g_i(0))\right)+\frac{e^{\eta t}-1}{\eta}\kappa_1(q).$$

Furthermore,

$$\begin{aligned}\limsup_{t\to\infty}\mathbb{E}\left[|(F,P,H)|^q\right]&\leq 3^{\frac{q}{2}}q\lim_{t\to\infty}\mathbb{E}\left(V_1(F,P,H,g_i)\right)\\ &\leq 3^{\frac{q}{2}}q\lim_{t\to\infty}\mathbb{E}\left[\frac{V_1(F(0),P(0),H(0),g_i(0))}{e^{\eta t}}+\frac{e^{\eta t}-1}{\eta e^{\eta t}}\kappa_1(q)\right]\\ &=3^{\frac{q}{2}}\frac{q\kappa_1(q)}{\eta}:=\kappa_2(q).\end{aligned} \tag{3.14}$$

Let $Q(q)=\kappa_2(q)$, which completes the proof of Lemma 3.1.

□

Theorem 3.2. *The solutions to system* (1.2) *exhibit stochastic ultimate boundedness.*

Proof. Based on the above derivation process, we can conclude that when $q=\frac{1}{2}$, $Q(q)$ satisfies $\limsup_{t\to\infty}\mathbb{E}\sqrt{|(F,P,H)|}\leqslant Q(q)$. Applying Chebyshev's inequality, for any $\varepsilon>0$, let $\varpi=\frac{\sqrt{3}\kappa_1\left(\frac{1}{2}\right)^2}{4\varepsilon^2\eta^2}$. We can then derive that

$$P(|(F,P,H)|>\varpi)\leqslant\frac{\mathbb{E}\left[\sqrt{|(F,P,H)|}\right]}{\sqrt{\varpi}}.$$

From the above equation, we can derive: $\limsup_{t\to\infty}P(|(F,P,H)|>\varpi)\leqslant\frac{Q}{\frac{Q}{\varepsilon}}=\varepsilon$. Combining this with the content of Definition 3.1 completes the proof of Theorem 3.2. □

3.3. Existence of a stationary distribution

In the study of biological systems, clarifying the long-term dynamic evolution of systems under random influences is crucial. The core focus of such analysis lies in determining whether the system possesses a stationary distribution that characterizes its long-term probabilistic behavior. Establishing sufficient conditions for the existence of a stationary distribution aids in predicting the survival status and stability of populations over time. According to Theorem 3.1, the system (1.2) possesses a globally unique solution. Therefore, the domain $\mathbb{R}^m$ in Lemma 2.1 should be replaced with $\mathbb{R}^3_+ \times \mathbb{R}^3$.

Theorem 3.3. *Let N be a positive number satisfying $N \in \left(\max\left\{0, \frac{2+\Pi_1}{\sum_{i=1}^3 \overline{g_i}}\right\}, \frac{c}{4a_2}\right)$, where*

$$\Pi_1 = \sup_{(F,P,H,g_i)\in\mathbb{R}^3_+\times\mathbb{R}^3} \left\{ \left(|g_1| + \frac{Ng_1}{K} + \frac{(a_1+\alpha_1)}{\beta}\right)F - e^{g_2}P - e^{g_3}H - \frac{|g_1|}{K}F^2 + \frac{1}{2}F^{\frac{4}{3}} + \left(\frac{1}{2}+\alpha_2\right)H \right.$$
$$\left. + N\left(e^{g_2} + e^{g_3} + g_2 + g_3\right) - \frac{a_2FH}{c+F} + \sum_{i=1}^{3}\left(\frac{3}{2}g_i^2\sigma_i^2 + g_i^3\beta_i(\overline{g_i} - g_i)\right)\right\}$$

Then, for any initial values $(F(0), P(0), H(0), g_i(0))$ belonging to $\mathbb{R}^3_+ \times \mathbb{R}^3$, the system (1.2) *possesses a stationary distribution on $\mathbb{R}^3_+ \times \mathbb{R}^3$.*

Proof. Define the Lyapunov function V_2 mapping from $\mathbb{R}^3_+ \times \mathbb{R}^3$ to $\mathbb{R}$ as follows:

$$V_2 = N\left(-\ln F - \ln P - \ln H - \sum_{i=1}^{3}\frac{g_i}{\beta_i}\right) + F + P + H + \sum_{i=1}^{3}\frac{g_i^4}{4}.$$

Applying Itô's formula to the function V_2 and combining it with the definition of N yields:

$$
\begin{aligned}
\mathcal{L}V_2 &= (F-N)\left[g_1\left(1-\frac{F}{K}\right)+\frac{a_1P}{1+\alpha F+\beta P+\gamma H}-\frac{a_2H}{c+F}\right]+(P-N)\left[\frac{\alpha_1F}{1+\alpha F+\beta P+\gamma H}-e^{g_2}\right]\\
&\quad+(H-N)\left[\frac{\alpha_2F}{c+F}-e^{g_3}\right]-N\sum_{i=1}^{3}(\overline{g_i}-g_i)+\sum_{i=1}^{3}\left(\frac{3}{2}g_i^2\sigma_i^2+g_i^3\beta_i(\overline{g_i}-g_i)\right)\\
&\leq -N\sum_{i=1}^{3}\overline{g_i}+\left(|g_1|+\frac{Ng_1}{K}\right)F-e^{g_2}P-e^{g_3}H-\frac{|g_1|}{K}F^2+\frac{1}{2}F^{\frac{4}{3}}+\frac{1}{2}H+N\left(e^{g_2}+e^{g_3}+g_2+g_3\right)\\
&\quad-\frac{a_2FH}{c+F}+\frac{(a_1+\alpha_1)FP}{1+\alpha H+\beta P+\gamma H}+\frac{\alpha_2FH}{c+F}+\sum_{i=1}^{3}\left(\frac{3}{2}g_i^2\sigma_i^2+g_i^3\beta_i(\overline{g_i}-g_i)\right)\\
&\quad+N\left(\frac{a_2H}{c+F}-\frac{a_1P}{1+\alpha F+\beta P+\gamma H}-\frac{\alpha_1F}{1+\alpha F+\beta P+\gamma H}-\frac{\alpha_2F}{c+F}\right)\\
&\quad-\frac{1}{2}F^{\frac{4}{3}}-\frac{1}{2}H-\frac{1}{2}\sum_{i=1}^{3}\beta_ig_i^4\\
&\leq -N\sum_{i=1}^{3}\overline{g_i}+\left(|g_1|+\frac{Ng_1}{K}+\frac{(a_1+\alpha_1)}{\beta}\right)F-e^{g_2}P-e^{g_3}H-\frac{|g_1|}{K}F^2+\frac{1}{2}F^{\frac{4}{3}}+\left(\frac{1}{2}+\alpha_2\right)H\\
&\quad+N\left(e^{g_2}+e^{g_3}+g_2+g_3\right)-\frac{a_2FH}{c+F}+\sum_{i=1}^{3}\left(\frac{3}{2}g_i^2\sigma_i^2+g_i^3\beta_i(\overline{g_i}-g_i)\right)\\
&\quad+N\left(\frac{a_2H}{c+F}-\frac{a_1P}{1+\alpha F+\beta P+\gamma H}-\frac{\alpha_1F}{1+\alpha F+\beta P+\gamma H}-\frac{\alpha_2F}{c+F}\right)\\
&\quad-\frac{1}{2}F^{\frac{4}{3}}-\frac{1}{2}H-\frac{1}{2}\sum_{i=1}^{3}\beta_ig_i^4.
\end{aligned}
$$

Then,

$$
\begin{aligned}
\mathcal{L}V_2 \leqslant\ & -2+N\left(\frac{a_2H}{c+F}-\frac{a_1P}{1+\alpha F+\beta P+\gamma H}-\frac{\alpha_1F}{1+\alpha F+\beta P+\gamma H}-\frac{\alpha_2F}{c+F}\right)\\
&-\frac{1}{2}F^{\frac{4}{3}}-\frac{1}{2}H-\frac{1}{2}\sum_{i=1}^{3}\beta_ig_i^4.
\end{aligned}
\tag{3.15}
$$

From the given expression of $V_2(F,P,H,g_1,g_2,g_3)$, it can be seen that as F and P approach infinity, the function $V_2(F,P,H,g_1,g_2,g_3)$ also approaches infinity. Therefore, within $\mathbb{R}^3_+\times\mathbb{R}^3$, there exists a point $(F^0,P^0,H^0,g_1^0,g_2^0,g_3^0)$ where $V_2(F,P,H,g_1,g_2,g_3)$ attains its minimum value. Combining the previous analysis with the functional conditions listed in Lemma 2.1, we can define a non-negative C^2 - function $V_3(F,P,H,g_1,g_2,g_3)$ with the following expression:

$$
V_3(F,P,H,g_1,g_2,g_3)=V_2(F,P,H,g_1,g_2,g_3)-V_2\left(F^0,P^0,H^0,g_1^0,g_2^0,g_3^0\right).
$$

Applying Itô's formula to $V_2(F,P,H,g_1,g_2,g_3)$ reveals that adding the constant term $V_2(F^0,P^0,H^0,g_1^0,g_2^0,g_3^0)$ to this function does not affect the final expression. Therefore, the functions $V_2(F,P,H,g_1,g_2,g_3)$ and $V_3(F,P,H,g_1,g_2,g_3)$ are governed by the same operator, leading to the

following inequality:

$$\begin{aligned}\mathcal{L}V_3 \leqslant -2 + N\left(\frac{a_2H}{c+F} - \frac{a_1P}{1+\alpha F+\beta P+\gamma H} - \frac{\alpha_1F}{1+\alpha F+\beta P+\gamma H} - \frac{\alpha_2F}{c+F}\right)\\ - \frac{1}{2}F^{\frac{4}{3}} - \frac{1}{2}H - \frac{1}{2}\sum_{i=1}^{3}\beta_i g_i^4.\end{aligned} \tag{3.16}$$

We select a closed set $\mathbb{H}_\varepsilon$ defined as follows:

$$\mathbb{H}_\varepsilon = \left\{(F,P,H,g_i) \in \mathbb{R}_+^3 \times \mathbb{R}^3 \,\middle|\, F \in \left[\varepsilon^3, \frac{1}{\varepsilon^3}\right],\ P \in \left[\varepsilon^4, \frac{1}{\varepsilon^4}\right],\ H \in \left[\varepsilon^4, \frac{1}{\varepsilon^4}\right],\ g_i \in \left[-\frac{1}{\varepsilon}, \frac{1}{\varepsilon}\right]\right\},$$

and denote Π_2 as

$$\begin{aligned}\Pi_2 = \sup_{(F,P,H,g_i)\in\mathbb{R}_+^3\times\mathbb{R}^3} \left\{N\left(\frac{a_2H}{c+F} - \frac{a_1P}{1+\alpha F+\beta P+\gamma H} - \frac{\alpha_1F}{1+\alpha F+\beta P+\gamma H} - \frac{\alpha_2F}{c+F}\right)\right.\\ \left. - \frac{1}{4}F^{\frac{4}{3}} - \frac{1}{4}H - \frac{1}{4}\sum_{i=1}^{3}\beta_i g_i^4.\right\}\end{aligned}$$

Set a sufficiently small value $\varepsilon \in (0,1)$ such that the following inequality holds:

$$-2 + \Pi_2 - \frac{\min\{1,\beta_i\}}{4}\left(\frac{1}{\varepsilon}\right)^4 \leqslant -1,\ i = 1,2,3. \tag{3.17}$$

$$-2 + \frac{Na_2}{c}\varepsilon^4 \leqslant -1\,. \tag{3.18}$$

We can decompose the complement of this closed set into nine mutually exclusive regions, specifically expressed as $(\mathbb{R}_+^3 \times \mathbb{R}^3) \setminus \mathbb{H}_\varepsilon = \bigcup_{k=1}^{9} \mathbb{H}_{k,\varepsilon}^c$, where

$$\mathbb{H}_{1,\varepsilon}^c = \left\{(F,P,H,g_i) \in \mathbb{R}_+^3 \times \mathbb{R}^3 \,\middle|\, F \in \left(\frac{1}{\varepsilon^3}, \infty\right)\right\},$$

$$\mathbb{H}_{2,\varepsilon}^c = \left\{(F,P,H,g_i) \in \mathbb{R}_+^3 \times \mathbb{R}^3 \,\middle|\, H \in \left(\frac{1}{\varepsilon^4}, \infty\right)\right\},$$

$$\mathbb{H}_{3,\varepsilon}^c = \left\{(F,P,H,g_i) \in \mathbb{R}_+^3 \times \mathbb{R}^3 \,\middle|\, P \in \left(\frac{1}{\varepsilon^4}, \infty\right)\right\},$$

$$\mathbb{H}_{j,\varepsilon}^c = \left\{(F,P,H,g_i) \in \mathbb{R}_+^3 \times \mathbb{R}^3 \,\middle|\, |g_i| \in \left(\frac{1}{\varepsilon}, \infty\right)\right\},\ j = 4,5,6;\ i = 1,2,3,$$

$$\mathbb{H}_{7,\varepsilon}^c = \left\{(F,P,H,g_i) \in \mathbb{R}_+^3 \times \mathbb{R}^3 \,\middle|\, F \in \left(0, \varepsilon^3\right)\right\},$$

$$\mathbb{H}_{8,\varepsilon}^c = \left\{(F,P,H,g_i) \in \mathbb{R}_+^3 \times \mathbb{R}^3 \,\middle|\, H \in \left(0, \varepsilon^4\right)\right\},$$

$$\mathbb{H}_{9,\varepsilon}^c = \left\{(F,P,H,g_i) \in \mathbb{R}_+^3 \times \mathbb{R}^3 \,\middle|\, P \in \left(0, \varepsilon^4\right)\right\}.$$

Next, we will prove that for any (F,P,H,g_i) belonging to $(\mathbb{R}_+^3 \times \mathbb{R}^3) \setminus \mathbb{H}_\varepsilon$, the inequality $\mathcal{L}V_3 \leqslant -1$ holds. Based on the partition of the complement described above, we can complete this proof by

considering five distinct cases.

Case 1. If $(F, P, H, g_i) \in \mathbb{H}^c_{1,\varepsilon}$, combining Eq (3.16) with Eq (3.17) yields the corresponding result, leading to the following inequality:

$$\mathcal{L}V_3 \leqslant -2 + \Pi_2 - \frac{1}{4}F^{\frac{4}{3}} \leqslant -2 + \Pi_2 - \frac{1}{4}\left(\frac{1}{\varepsilon}\right)^4 \leqslant -1.$$

Case 2. If $(F, P, H, g_i) \in \mathbb{H}^c_{2,\varepsilon}$, then combining Eq (3.16) with Eq (3.17) yields

$$\mathcal{L}V_3 \leqslant -2 + \Pi_2 - \frac{1}{4}H \leqslant -2 + \Pi_2 - \frac{1}{4}\left(\frac{1}{\varepsilon}\right)^4 \leqslant -1.$$

Case 3. If $(F, P, H, g_i) \in \mathbb{H}^c_{3,\varepsilon}$ and $(F, P, H, g_i) \in \mathbb{H}^c_{7,\varepsilon}$ and $(F, P, H, g_i) \in \mathbb{H}^c_{9,\varepsilon}$, then by deriving through Eq (3.16), we obtain

$$\mathcal{L}V_3 \leqslant -2 - \left(\frac{1}{4} - \frac{Na_2}{c}\right)H \leqslant -2 \leqslant -1.$$

Case 4. If $(F, P, H, g_i) \in \mathbb{H}^c_{j,\varepsilon}$, expanding the derivation based on Eqs (3.16) and (3.17) yields

$$\mathcal{L}V_3 \leqslant -2 + \Pi_2 - \frac{\beta_i}{4}g_i^4 \leqslant -2 + \Pi_2 - \frac{\beta_i}{4}\left(\frac{1}{\varepsilon}\right)^4 \leqslant -1, \forall\ j = 4, 5, 6, \forall i = 1, 2, 3.$$

Case 5. If $(F, P, H, g_i) \in \mathbb{H}^c_{8,\varepsilon}$, then by deriving from Eqs (3.16) and (3.18), we obtain

$$\mathcal{L}V_3 \leqslant -2 + \frac{Na_2}{c}H \leqslant -2 + \frac{Na_2}{c}\varepsilon^4 \leqslant -1.$$

Thus, we can prove that there exists a sufficiently small constant ε such that for all (F, P, H, g_i) falling within $(\mathbb{R}^3_+ \times \mathbb{R}^3) \setminus \mathbb{H}_\varepsilon$, the inequalities $\mathcal{L}V_3(F, P, H, g_i) \leq -1$ holds. Here, ε must satisfy the following condition:

$$\varepsilon \leqslant \min\left\{1, \sqrt[4]{\frac{c}{Na_2}}\right\},$$

For any case where $\Pi_2 \leqslant 1$, this holds true. Additionally, for any case where $\Pi_2 > 1$, ε must satisfy:

$$\varepsilon \leqslant \min\left\{1, \sqrt[4]{\frac{\min\{1, \beta_1, \beta_2, \beta_3\}}{4(\Pi_2 - 1)}}\right\}.$$

□

3.4. Extinction

Theorem 3.4. *We define*

$$\varphi_1(t) = \bar{r} - \varepsilon\frac{\phi_1^2}{4\eta_1}, \bar{\varphi}_1 = \lim_{t\to\infty}\frac{1}{t}\int_0^t \varphi_1(s)ds = \bar{r} - \varepsilon\frac{\phi_1^2}{4\eta_1},$$
$$\varphi_2(t) = -\bar{d}_1 - \frac{\phi_2^2}{4\eta_2} + \frac{\phi_2^2}{4\eta_2}e^{-2\eta_2 t}, \bar{\varphi}_2 = \lim_{t\to\infty}\frac{1}{t}\int_0^t \varphi_2(s)ds = -\bar{d}_1 - \frac{\phi_2^2}{4\eta_2},$$
$$\varphi_3(t) = -\bar{d}_2 - \frac{\phi_3^2}{4\eta_3} + \frac{\phi_3^2}{4\eta_3}e^{-2\eta_3 t}, \bar{\varphi}_3 = \lim_{t\to\infty}\frac{1}{t}\int_0^t \varphi_3(s)ds = -\bar{d}_2 - \frac{\phi_3^2}{4\eta_3}.$$

When $\bar{\varphi}_1 + \frac{a_1}{\beta} < 0$, $\bar{\varphi}_2 + \frac{\alpha_1}{\alpha} < 0$, $\bar{\varphi}_3 + \alpha_2 < 0$, *then* $F(t), P(t), H(t)$ *are extinct.*

Proof. By combining Eq (1.2) with the definition of the Ornstein-Uhlenbeck process, we can derive that

$$\begin{aligned} r &= \bar{r} + [r(0) - \bar{r}]e^{-\eta_1 t} + \phi_1 \int_0^t e^{-\eta_1(t-s)} dB_1(s), \\ d_1 &= \bar{d}_1 + [d_1(0) - \bar{d}_1]e^{-\eta_2 t} + \phi_2 \int_0^t e^{-\eta_2(t-s)} dB_2(s), \\ d_2 &= \bar{d}_2 + [d_2(0) - \bar{d}_2]e^{-\eta_3 t} + \phi_3 \int_0^t e^{-\eta_3(t-s)} dB_3(s), \end{aligned} \tag{3.19}$$

where η_i and ϕ_i are positive constants, $i = 1, 2, 3$; η_i represents the recovery rate, and ϕ_i represents the volatility intensity. Equation (3.19) indicates that within the interval $[0, t]$, $r(t)$, $d_1(t)$, and $d_2(t)$ follow normal distributions $\mathbb{N}(\mathbb{E}[r(t)], \mathbb{VAR}[r(t)])$, $\mathbb{N}(\mathbb{E}[d_1(t)], \mathbb{VAR}[d_1(t)])$, and $\mathbb{N}(\mathbb{E}[d_2(t)], \mathbb{VAR}[d_2(t)])$, respectively. From this, we can derive the following:

$$\mathbb{E}[r(t)] = \bar{r} + [r(0) - \bar{r}]e^{-\eta_1 t}, \mathbb{VAR}[r(t)] = \frac{\phi_1^2}{2\eta_1}\left(1 - e^{-2\eta_1 t}\right),$$

$$\mathbb{E}[d_1(t)] = \bar{d}_1 + [d_1(0) - \bar{d}_1]e^{-\eta_2 t}, \mathbb{VAR}[d_1(t)] = \frac{\phi_2^2}{2\eta_2}\left(1 - e^{-2\eta_2 t}\right),$$

$$\mathbb{E}[d_2(t)] = \bar{d}_2 + [d_2(0) - \bar{d}_2]e^{-\eta_3 t}, \mathbb{VAR}[d_2(t)] = \frac{\phi_3^2}{2\eta_3}\left(1 - e^{-2\eta_3 t}\right).$$

Therefore, for each $i = 1, 2, 3$, the terms $\phi_i \int_0^t e^{-\eta_i(t-s)} dB_i(s)$ follows a normal distribution $\mathbb{N}\left(0, \frac{\phi_i^2}{2\eta_i}\left(1 - e^{-2\eta_i t}\right)\right)$. This expression can also be equivalently written as $\frac{\phi_i}{\sqrt{2\eta_i}}\sqrt{1 - e^{-2\eta_i t}}\frac{dB_i(t)}{dt}$. Based on this, we define $\gamma_i(t) = \frac{\phi_i}{\sqrt{2\eta_i}}\sqrt{1 - e^{-2\eta_i t}}$, where $B_i(t)$ denotes standard Brownian motion. Consequently, Eq (3.19) can be rewritten as follows:

$$\begin{aligned} r &= \bar{r} + [r(0) - \bar{r}]e^{-\eta_1 t} + \gamma_1 \frac{dB_1(t)}{dt}, \\ d_1 &= \bar{d}_1 + [d_1(0) - \bar{d}_1]e^{-\eta_2 t} + \gamma_2 \frac{dB_2(t)}{dt}, \\ d_2 &= \bar{d}_2 + [d_2(0) - \bar{d}_2]e^{-\eta_3 t} + \gamma_3 \frac{dB_3(t)}{dt}. \end{aligned} \tag{3.20}$$

Following this, we proceed to refine the system (1.2) accordingly:

$$\begin{cases} dF(t) = F(t)\left((\bar{r} + [r(0) - \bar{r}]e^{-\eta_1 t})\left(1 - \frac{F(t)}{K}\right) + \frac{a_1 P(t)}{1+\alpha F(t)+\beta P(t)+\gamma H(t)} - \frac{a_2 H(t)}{c+F(t)}\right)dt + \left(1 - \frac{F(t)}{K}\right)\gamma_1 F(t) dB_1(t), \\ dP(t) = P(t)\left(-\left(\bar{d}_1 + [d_1(0) - \bar{d}_1]e^{-\eta_2 t}\right) + \frac{\alpha_1 F(t)}{1+\alpha F(t)+\beta P(t)+\gamma H(t)}\right)dt - \gamma_2 P(t) dB_2(t), \\ dH(t) = H(t)\left(-\left(\bar{d}_2 + [d_2(0) - \bar{d}_2]e^{-\eta_3 t}\right) + \frac{\alpha_2 F(t)}{c+F(t)}\right)dt - \gamma_3 H(t) dB_3(t). \end{cases} \tag{3.21}$$

Applying Itô's formula to $\ln F(t)$, $\ln P(t)$, and $\ln H(t)$, and integrating over the interval $[0, t]$, we obtain the following results:

$$\ln F(t) = \ln F(0) + \int_0^t (\bar{r} + [r(0) - \bar{r}]e^{-\eta_1 s})\left(1 - \frac{F(s)}{K}\right)ds + \int_0^t \frac{a_1 P(s)}{1 + \alpha F(s) + \beta P(s) + \gamma H(s)}ds - \int_0^t \frac{a_2 H(s)}{c + F(s)}ds$$
$$- \int_0^t \frac{\phi_1^2}{4\eta_1}\left(1 - e^{-2\eta_1 s}\right)\left(1 - \frac{F(s)}{K}\right)^2 ds + \int_0^t \left(1 - \frac{F(s)}{K}\right)\gamma_1(s)dB_1(s),$$

$$\begin{aligned}\ln P(t) &= \ln P(0) + \int_0^t \varphi_2(s)ds + \int_0^t \frac{\alpha_1 F(s)}{1 + \alpha F(s) + \beta P(s) + \gamma H(s)}ds \\ &\quad - \frac{d_1(0) - \bar{d}_1}{\eta_2}\left(1 - e^{-\eta_2 t}\right) - \int_0^t \gamma_2(s)dB_2(s), \\ \ln H(t) &= \ln H(0) + \int_0^t \varphi_3(s)ds + \int_0^t \frac{\alpha_2 F(s)}{c + F(s)}ds \\ &\quad - \frac{d_2(0) - \bar{d}_2}{\eta_3}\left(1 - e^{-\eta_3 t}\right) - \int_0^t \gamma_3(s)dB_3(s).\end{aligned} \tag{3.22}$$

Given that $\bar{r}$ can be either positive or negative, we will separately examine the cases where $\bar{r} \leqslant 0$ and $\bar{r} > 0$. When $\bar{r} > 0$, we obtain $0 \leqslant \lim_{t\to\infty} \frac{1}{t}\int_0^t \bar{r}\left(1 - e^{-\eta_1 s}\right)\left(1 - \frac{F(s)}{K}\right)ds \leqslant \bar{r}$, and for any $\varepsilon > 0$, we have

$$\frac{1}{t}\ln\frac{F(t)}{F(0)} \leqslant \frac{1}{t}\int_0^t \left(\bar{r} - \varepsilon\frac{\phi_1^2}{4\eta_1}\right)ds + \frac{r(0)}{t\eta_1}\left(1 - e^{-\eta_1 t}\right) + \frac{\varepsilon\phi_1^2}{4\eta_1}\left(1 - \frac{1}{2\eta_1}e^{-2\eta_1 t}\right) + \frac{a_1}{\beta} + \frac{1}{t}\int_0^t \left(1 - \frac{F(s)}{K}\right)\gamma_1(s)dB_1(s).$$

By Lemma 2.2, $\int_0^t \gamma_i(s)dB_i(s)$ satisfies the strong law of large numbers for martingales, implying that $\lim_{t\to\infty} \frac{1}{t}\int_0^t \gamma_i(s)dB_i(s) = 0$. It follows that

$$\limsup_{t\to\infty} \frac{\ln F(t)}{t} \leqslant \bar{\varphi}_1 + \frac{a_1}{\beta}.$$

In the process of analyzing P and H, we can derive from Eq (3.22) that

$$\begin{cases} t^{-1}\ln\frac{P(t)}{P(0)} \leqslant \bar{\varphi}_2 - \frac{d_1(0) - \bar{d}_1}{t\eta_2}\left(1 - e^{-\eta_2 t}\right) + \frac{\alpha_1}{\alpha} - \frac{1}{t}\int_0^t \gamma_2(s)dB_2(s), \\ t^{-1}\ln\frac{H(t)}{H(0)} \leqslant \bar{\varphi}_3 - \frac{d_2(0) - \bar{d}_2}{t\eta_3}\left(1 - e^{-\eta_3 t}\right) + \alpha_2 - \frac{1}{t}\int_0^t \gamma_3(s)dB_3(s). \end{cases} \tag{3.23}$$

Taking the upper limit simultaneously at both ends of Eq (3.23), we obtain

$$\begin{cases} \limsup_{t\to\infty} \frac{\ln P(t)}{t} \leqslant \bar{\varphi}_2 + \frac{\alpha_1}{\alpha}, \\ \limsup_{t\to\infty} \frac{\ln H(t)}{t} \leqslant \bar{\varphi}_3 + \alpha_2. \end{cases} \tag{3.24}$$

According to the strong law of large numbers and the definition of the Ornstein-Uhlenbeck process, if $\bar{\varphi}_1 + \frac{a_1}{\beta} < 0$, then $\lim_{t\to\infty} F(t) = 0$. Similarly, when $\bar{\varphi}_2 + \frac{\alpha_1}{\alpha} < 0$ and $\bar{\varphi}_3 + \alpha_2 < 0$, we obtain $\lim_{t\to\infty} P(t) = 0$ and $\lim_{t\to\infty} H(t) = 0$. Thus, Theorem 3.4 is proven.

Remark 3.1. We emphasize that our model (1.2) describes population dynamics of plants, pollinators, and herbivores; there is no disease component. The term "extinction" throughout this section refers to

the eventual decline of a species population to zero, not disease eradication. The conditions $\bar{\varphi}_1 + \frac{a_1}{\beta} < 0$, $\bar{\varphi}_2 + \frac{\alpha_1}{\alpha} < 0$, and $\bar{\varphi}_3 + \alpha_2 < 0$ have clear biological interpretations: they imply that the long-term effective growth rate of each species, after accounting for environmental variability and interspecific interactions, becomes negative. For instance, $\bar{\varphi}_1 + \frac{a_1}{\beta} < 0$ means that even with maximum mutualistic benefit from pollinators, the plant's net intrinsic growth rate cannot sustain positive growth, leading to eventual extinction. These thresholds provide practical guidelines for conservation: if noise intensities or mean reversion speeds shift these quantities below zero, then extinction risk becomes certain.

□

4. Numerical simulations

In this section, we will conduct numerical simulations to validate the obtained results. Using the Euler-Maruyama method [46], we derive the discrete form of system (1.2) as follows:

$$\begin{cases} F^{j+1} = F^j + F^j\left(g_1^j\left(1-\dfrac{F^j}{K}\right) + \dfrac{a_1P^j}{1+\alpha F^j+\beta P^j+\gamma H^j} - \dfrac{a_2H^j}{c+F^j}\right)\Delta t, \\ P^{j+1} = P^j + P^j\left(\dfrac{\alpha_1F^j}{1+\alpha F^j+\beta P^j+\gamma H^j} - e^{g_2^j}\right)\Delta t, \\ H^{j+1} = H^j + H^j\left(\dfrac{\alpha_2F^j}{c+F^j} - e^{g_3^j}\right)\Delta t, \\ g_1^{j+1} = g_1^j + \beta_1\left(\overline{g}_1 - g_1^j\right)\Delta t + \sigma_1\sqrt{\Delta t}\omega_j, \\ g_2^{j+1} = g_2^j + \beta_2\left(\overline{g}_2 - g_2^j\right)\Delta t + \sigma_2\sqrt{\Delta t}\xi_j, \\ g_3^{j+1} = g_3^j + \beta_3\left(\overline{g}_3 - g_3^j\right)\Delta t + \sigma_3\sqrt{\Delta t}\zeta_j, \end{cases} \tag{4.1}$$

Here, $\Delta t > 0$ represents the time increment and ω_j, ξ_j, ζ_j denote three independent random variables each following a standard Gaussian distribution $\mathbb{N}(0,1)$. Furthermore, (F^j, P^j, H^j, g_i^j) corresponds to the numerical values obtained at iteration j for the discretized Eq (4.1), where $i = 1, 2, 3$ and $j = 1, 2, \ldots$. We selected multiple combinations of biological parameters from Tables 1 and 2 for computation. Specifically, the plant carrying capacity K, the half-saturation constant $c = 90$, and the maximum feeding rates a_1, a_2 are consistent with empirical measurements of temperate grassland ecosystems. The mortality rates e^{g_2}, e^{g_3} and plant growth rate g_1 fall within biologically realistic ranges for annual plants and insects. The Beddington-DeAngelis coefficients $\alpha = 0.5, \beta = 0.4, \gamma = 0.5$ are chosen to reflect moderate handling time, pollinator interference, and varying levels of herbivore disturbance, respectively. Thus, all simulations are grounded in realistic ecological contexts.

Table 1. List of biological parameters in system (1.2).

Parameter	Description
$\overline{g}_1$	Average growth rate of the plants
$\overline{g}_2$	Average log-transformed natural mortality rate of the pollinators
$\overline{g}_3$	Average log-transformed natural mortality rate of the herbivores
K	Environmental carrying capacity of the plants
a_1	Maximum feeding rate of pollinators on plants
a_2	Maximum feeding rate of herbivores on plants
α_1	Conversion efficiency of plants transforming into pollinators
α_2	Conversion efficiency of plants into herbivore growth
α	Time cost coefficient for pollinator processing of plants
β	Time waste coefficient during encounters among pollinators
γ	Herbivore disturbance intensity coefficient for pollinators
c	Half-saturation constant for the plants
β_1	Reversion speed of g_1
β_2	Reversion speed of g_2
β_3	Reversion speed of g_3
σ_1	Volatility intensity of g_1
σ_2	Volatility intensity of g_2
σ_3	Volatility intensity of g_3

Based on the biological significance of the parameters in Table 1 and Jørgensen's real dataset [47], we constructed Table 2 by selecting data related to plants, pollinators, and herbivores. The explicit predator-prey relationships among these three groups reflect energy transfer and interaction processes within the food chain model, thereby enabling verification of the model properties demonstrated earlier.

Table 2. Several combinations of biological parameters of the system.

Combinations	Value
$(\mathcal{A}_1)$	$\overline{g}_1 = 0.47, \overline{g}_2 = \log(0.25), \overline{g}_3 = \log(0.2), \beta_1 = 0.8, \beta_2 = 0.45, \beta_3 = 0.65, \sigma_1 = 0.02, \sigma_2 = 0.05$ $\sigma_3 = 0.03, K = 180, \alpha = 0.5, \beta = 0.4, \gamma = 2, c = 90, a_1 = 0.41, a_2 = 0.37, \alpha_1 = 0.35, \alpha_2 = 0.31$
$(\mathcal{A}_2)$	$\overline{g}_1 = 0.29, \overline{g}_2 = \log(0.2), \overline{g}_3 = \log(0.25), \beta_1 = 0.8, \beta_2 = 0.6, \beta_3 = 0.7, \sigma_1 = 0.03, \sigma_2 = 0.03$ $\sigma_3 = 0.04, K = 80, \alpha = 0.5, \beta = 0.4, \gamma = 2, c = 90, a_1 = 0.21, a_2 = 0.37, \alpha_1 = 0.47, \alpha_2 = 0.51$
$(\mathcal{A}_3)$	$\overline{g}_1 = 0.3, \overline{g}_2 = \log(0.23), \overline{g}_3 = \log(0.2), \beta_1 = 0.8, \beta_2 = 0.7, \beta_3 = 0.7, \sigma_1 = 0.03, \sigma_2 = 0.02$ $\sigma_3 = 0.02, K = 180, \alpha = 0.5, \beta = 0.4, \gamma = 2, c = 90, a_1 = 0.21, a_2 = 0.37, \alpha_1 = 0.4, \alpha_2 = 0.31$
$(\mathcal{A}_4)$	$\overline{g}_1 = -0.1, \overline{g}_2 = \log(0.7), \overline{g}_3 = \log(0.25), \beta_1 = 0.1, \beta_2 = 0.1, \beta_3 = 0.1, \sigma_1 = 0.01, \sigma_2 = 0.01$ $\sigma_3 = 0.01, K = 180, \alpha = 0.6, \beta = 0.4, \gamma = 0.5, c = 90, a_1 = 0.5, a_2 = 0.37, \alpha_1 = 0.35, \alpha_2 = 0.3$
$(\mathcal{A}_5)$	$\overline{g}_1 = 0.4, \overline{g}_2 = \log(0.7), \overline{g}_3 = \log(0.25), \beta_1 = 0.1, \beta_2 = 0.1, \beta_3 = 0.1, \sigma_1 = 0.01, \sigma_2 = 0.01$ $\sigma_3 = 0.01, K = 180, \alpha = 0.6, \beta = 0.4, \gamma = 0.5, c = 90, a_1 = 0.5, a_2 = 0.37, \alpha_1 = 0.35, \alpha_2 = 0.3$
$(\mathcal{A}_6)$	$\overline{g}_1 = 0.5, \overline{g}_2 = \log(0.7), \overline{g}_3 = \log(0.3), \beta_1 = 0.1, \beta_2 = 0.1, \beta_3 = 0.1, \sigma_1 = 0.01, \sigma_2 = 0.01$ $\sigma_3 = 0.01, K = 180, \alpha = 0.6, \beta = 0.4, \gamma = 0.95, c = 90, a_1 = 0.5, a_2 = 0.37, \alpha_1 = 0.35, \alpha_2 = 0.5$
$(\mathcal{A}_7)$	$\overline{g}_1 = 0.5, \overline{g}_2 = \log(0.2), \overline{g}_3 = \log(0.2), \beta_1 = 0.1, \beta_2 = 0.1, \beta_3 = 0.1, \sigma_1 = 0.01, \sigma_2 = 0.01$ $\sigma_3 = 0.01, K = 180, \alpha = 0.5, \beta = 0.4, \gamma = 2, c = 90, a_1 = 0.41, a_2 = 0.37, \alpha_1 = 0.35, \alpha_2 = 0.31$

Example 4.1. In Table 2, we select the parameter set $(\mathcal{A}_1) - (\mathcal{A}_3)$ to represent the biological parameters of system (1.2). According to the conclusion of Theorem 3.1, system (1.2) possesses a unique global solution. We set the maximum iteration count to $T_{\max} = 2000$, ultimately obtaining the results shown in

Figure 1.

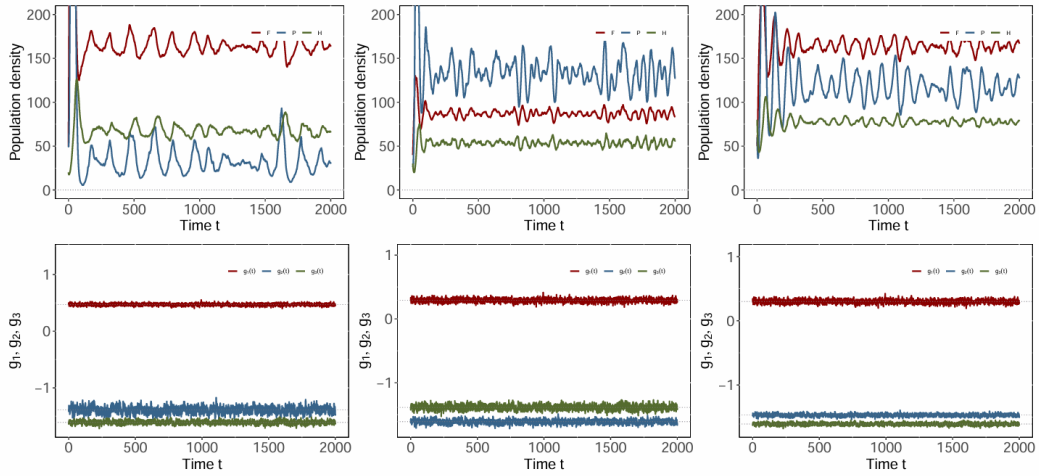

Figure 1. We conducted numerical simulations to analyze the dynamic characteristics of plants, pollinators, and herbivores in system (1.2). The resulting visualizations support Theorem 3.1, demonstrating that system (1.2) possesses a unique global solution determined by the parameter set $(\mathcal{A}_1) - (\mathcal{A}_3)$.

Remark 4.1. The results in Figure 1 show that the growth rate of F and the mortality rates of P and H fluctuate around their respective means, a characteristic reflecting the mean-reverting property of the Ornstein-Uhlenbeck process. Furthermore, different coefficient combinations yield distinct solutions, yet all solutions satisfy the conditions of existence and uniqueness. These findings provide empirical support for the conclusions of Theorem 3.1. Furthermore, different coefficient combinations yield distinct solutions, yet all solutions satisfy the conditions of existence and uniqueness. These findings provide empirical support for the conclusions of Theorem 3.1.

Example 4.2. To more clearly verify the existence and uniqueness of solutions to system (1.2), we conducted 100 simulation experiments based on Theorem 3.1. As shown in Figure 2, these 100 simulated trajectories were generated under identical initial conditions and parameter settings, with only minor random perturbations and the simulation duration set to $T_{\max} = 2000$.

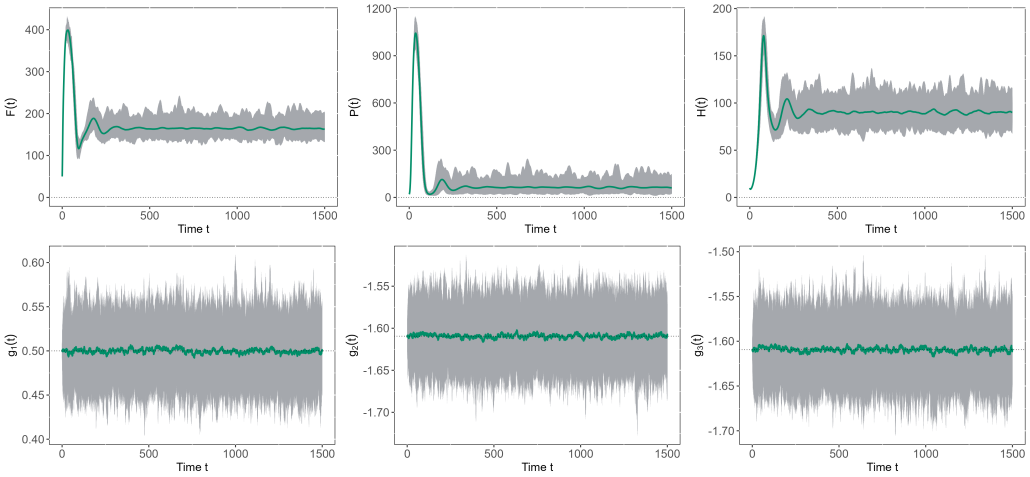

Figure 2. 100 path simulation figures.

Remark 4.2. In Figure 2, 100 simulated paths are depicted as gray lines, while the solid green line represents the average trajectory of these paths. It can be observed that different combinations of coefficients yield distinct solutions, and each solution possesses a unique form of existence. This result validates the conclusion of Theorem 3.1.

Example 4.3. In Table 2, the parameter sets $(\mathcal{A}_1) - (\mathcal{A}_3)$ are used to define the biological parameters of system (1.2). According to the conclusion of Lemma 3.1, the q-order moments of the solutions to system (1.2) are bounded, and the solutions themselves exhibit ultimate boundedness. We set the maximum iteration count to $T_{\max} = 2000$ and obtained the results presented in Figure 3.

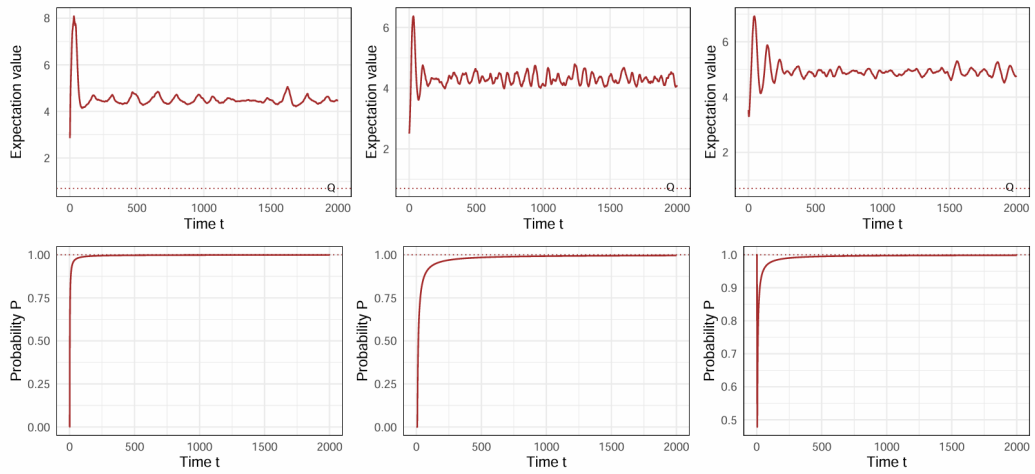

Figure 3. We conducted numerical simulations to investigate the dynamic characteristics of the qth-order moments of the solutions to system (1.2). The results indicate that the solutions remain bounded throughout, verifying the ultimate boundedness of the system. The relevant parameters used in the study were drawn from the parameter sets $(\mathcal{A}_1) - (\mathcal{A}_3)$.

Remark 4.3. Figure 3 shows that the expected values corresponding to the three coefficient combinations $(\mathcal{A}_1) - (\mathcal{A}_3)$ all lie below the finite upper bound $Q(q)$. As time t increases, the prob-

ability P gradually stabilizes and eventually exceeds a fixed threshold, specifically manifested as $\limsup_{t\to\infty} P\left(\sqrt{F^2(t)+P^2(t)+H^2(t)} \le \varpi\right) \ge 1-\varepsilon$. This observation validates the effectiveness of Theorem 3.2. From a biological perspective, this conclusion aligns with the reality that environmental resources are finite and no population can grow indefinitely.

Example 4.4. In Table 2, we employ the parameter combination ($\mathcal{A}_3$) to set the biological parameters of system (1.2). According to the conclusion of Theorem 3.3, the solutions of this system exhibit a stationary distribution. We set the iteration count to $T = 2000$ and obtained the simulation results shown in Figure 4.

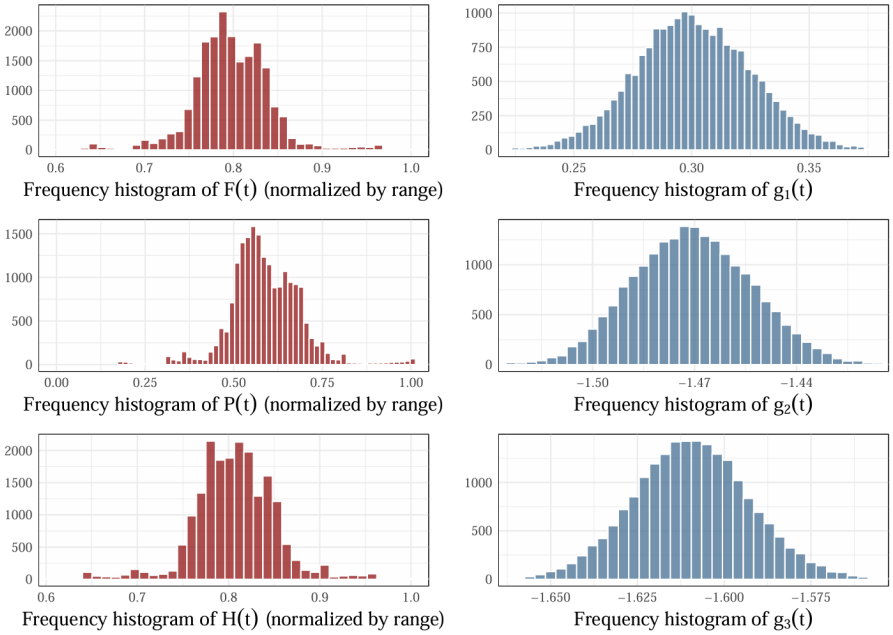

Figure 4. We conducted numerical simulations to analyze the stationary distribution of system (1.2). The results in Figure 4 show that the population size $F(t)$ primarily resides within the range of 0.7 to 0.9, $P(t)$ within 0.5 to 0.75, and $H(t)$ within 0.7 to 0.9. All population sizes are concentrated in the middle of their respective ranges. The frequency histograms of these populations exhibit a bimodal shape with a peak in the middle and tapered ends, resembling the form of a normal distribution. This indicates that even in the presence of random environmental disturbances, the growth state of the populations tends toward stability. The parameters used in this study are derived from the parameter combination ($\mathcal{A}_3$).

Example 4.5. To further validate the conclusions of Theorems 3.2 and 3.3, we employed the same methodology used to verify Theorem 3.1, conducting 100 path simulations. The results for the F population are shown in Figure 5. The left panel displays the simulation results for Theorem 3.2, while the right panel shows those for Theorem 3.3. It is evident that the conclusions of both theorems hold true.

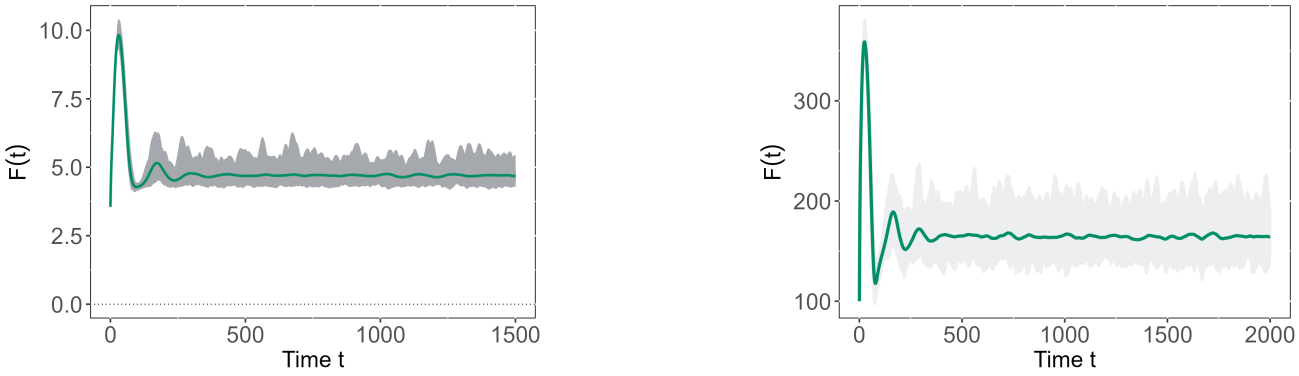

(a) 100 path simulation figure for Theorem 3.2

(b) 100 path simulation figure for Theorem 3.3

Figure 5. 100 path simulation figures for Theorems 3.2 and 3.3.

Remark 4.4. The 100-path simulations reinforce that Theorems 3.2 and 3.3 hold for a wide range of initial conditions. In ecological terms, even under persistent environmental fluctuations, the populations do not diverge to infinity and their long-term statistical behavior stabilizes. This justifies using the stationary distribution as a predictive tool for conservation planning.

Example 4.6. In Table 2, we selected the parameter combination $(\mathcal{A}_4) - (\mathcal{A}_7)$ to set the biological parameters of system (1.2). According to Theorem 3.4, system (1.2) will exhibit extinction behavior. We set the maximum iteration count to $T_{\max} = 2000$ and obtained the results presented in Figure 6.

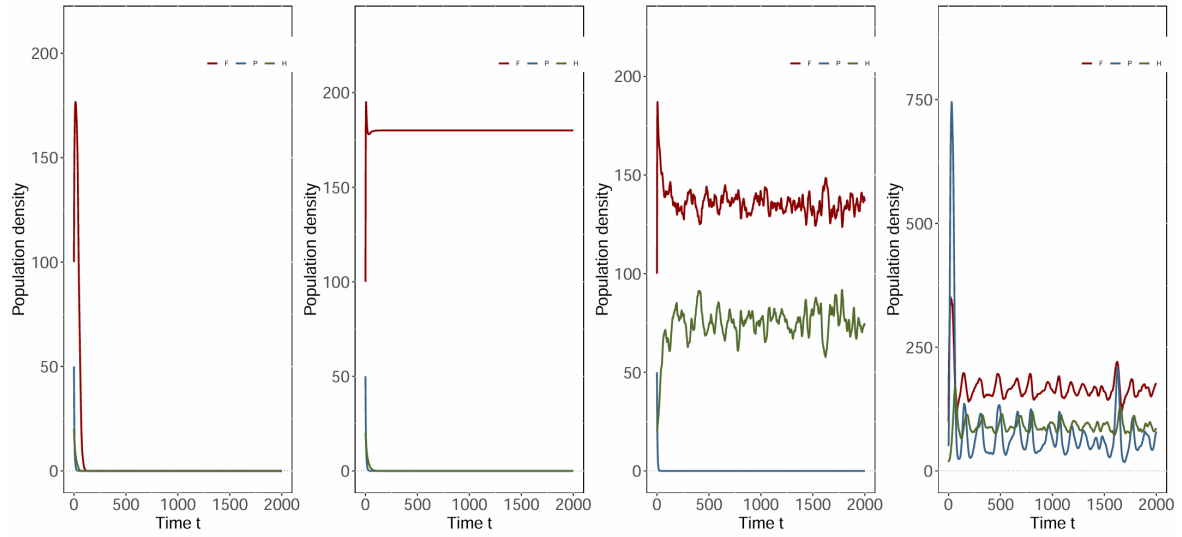

Figure 6. Through numerical simulations, we investigated the extinction behavior of system (1.2). When $\bar{\varphi}_1 + \frac{a_1}{\beta} < 0$, the F population will face extinction; when $\bar{\varphi}_2 + \frac{\alpha_1}{\alpha} < 0$, the P population will face extinction; and when $\bar{\varphi}_3 + \alpha_2 < 0$, the H population will face extinction. The relevant parameters employed in this study are determined by the parameter combinations $(\mathcal{A}_4) - (\mathcal{A}_7)$.

5. Conclusions

In this paper, we primarily investigate a stochastic predator-prey model driven by an OU process with Holling-II and BD composite functional responses. In the ecosystems frequently subjected to random environmental factors, the OU process with its mean-reverting characteristics accurately reflects the persistent and gradual nature of environmental fluctuations better than the traditional white noise assumption. This research provides a more reliable mathematical framework for understanding population dynamics under the combined influence of functional response patterns and stochastic disturbances. The main contributions of this paper are as follows:

We illustrate the biological basis for employing the OU process in modeling population survival under stochastic environments. We establish the existence and uniqueness of global solutions when analyzing the stochastic ultimate boundedness of this random model. By constructing appropriate Lyapunov functions and combining them with Itô's formula, we prove the existence of stationary distributions, thereby describing the stationary behavior of population persistence from a probabilistic perspective. Simultaneously, we provide sufficient conditions for the extinction of both predator and prey populations. Finally, numerical simulations not only validate the theoretical analysis but also further reveal how different functional response forms and random intensities jointly regulate the system's dynamic patterns and stability.

Overall, we extend the theoretical research on stochastic predator-prey models by integrating the OU process with two classical functional responses. These findings can help identify critical parameter thresholds determining population persistence or extinction, thereby offering theoretical guidance for predicting population dynamics and formulating intervention strategies in ecological conservation and management.

However, many unresolved issues remain worthy of further exploration. For instance, the model assumes parameters to be constant, whereas many factors in actual ecological environments, such as seasonal variations and resource cycles, exhibit periodicity or time-varying characteristics. Consequently, investigating stochastic systems with periodic coefficients or time-varying parameters would yield greater practical relevance. Furthermore, we only considers continuous fluctuations in environmental noise. In future work, researchers may incorporate mechanisms, such as the Lévy jump processes, to describe sudden environmental events, or account for time-delay effects to reflect memory and feedback in ecological processes. Consequently, the model would resemble the complexity of real ecosystems more closely.

Use of AI tools declaration

The authors declare they have not used Artificial Intelligence (AI) tools in the creation of this article.

Acknowledgments

This study was supported by the National Natural Science Foundation of China (Grant No.11401085), the Central University Basic Research Grant (2572021DJ04), the Heilongjiang Postdoctoral Grant (LBH-Q21059), the 2023 Project on Ideological and Political Education in Graduate Courses of Heilongjiang Province, Northeast Forestry University Educational Teaching Research Project (Graduate Student Special Project, No.DGYYJ2022-22).

Conflict of interest

The authors declare there is no conflicts of interest.

References

1. J. Memmott, N. M. Waser, M. V. Price, Tolerance of pollination networks to species extinctions, *Proc. R. Soc. B*, **271** (2004), 2605–2611. https://doi.org/10.1098/rspb.2004.2909
2. N. Mitani, A. Mougi, Population cycles emerging through multiple interaction types, *R. Soc. Open Sci.*, **4** (2017), 170536. https://doi.org/10.1098/rsos.170536
3. D. Xiao, S. Ruan, Multiple bifurcations in a delayed predator–prey system with nonmonotonic functional response, *J. Differ. Equations*, **176** (2001), 494–510. https://doi.org/10.1006/jdeq.2000.3982
4. R. Ramos-Jiliberto, A. A. Albornoz, F. S. Valdovinos, C. Smith-Ramírez, M. Arim, J. J. Armesto, et al., A network analysis of plant-pollinator interactions in temperate rain forests of Chiloé Island, Chile, *Oecologia*, **160** (2009), 697–706. https://doi.org/10.1007/s00442-009-1344-7
5. Y. Yacine, N. Loeuille, Stable coexistence in plant-pollinator-herbivore communities requires balanced mutualistic vs antagonistic interactions, *Ecol. Model.*, **465** (2022), 109857. https://doi.org/10.1016/j.ecolmodel.2021.109857
6. P. Turchin, *Quantitative Analysis of Movement: Measuring and Modeling Population Redistribution in Animals and Plants*, Sinauer Associates, Sunderland, MA, 1998.
7. L. Rustad, J. Campbell, G. Marion, R. Norby, M. Mitchell, A. Hartley, et al., A meta-analysis of the response of soil respiration, net nitrogen mineralization, and aboveground plant growth to experimental ecosystem warming, *Oecologia*, **126** (2001), 543–562. https://doi.org/10.1007/s004420000544
8. S. Y. Strauss, R. E. Irwin, Ecological and evolutionary consequences of multispecies plant-animal interactions, *Annu. Rev. Ecol. Evol. Syst.*, **35** (2004), 435–466. https://doi.org/10.1146/annurev.ecolsys.35.112202.130215
9. T. A. Revilla, T. Marcou, V. Křivan, Plant competition under simultaneous adaptation by herbivores and pollinators, *Ecol. Model.*, **455** (2021), 109634. https://doi.org/10.1016/j.ecolmodel.2021.109634
10. S. Y. Strauss, J. K. Conner, S. L. Rush, Foliar herbivory affects floral characters and plant attractiveness to pollinators: implications for male and female plant fitness, *Am. Nat.*, **147** (1996), 1098–1107. https://doi.org/10.1086/285896
11. R. S. Fritz, E. L. Simms (eds.), *Plant Resistance to Herbivores and Pathogens: Ecology, Evolution, and Genetics*, The University of Chicago Press, Chicago, 1992.
12. S. Y. Strauss, Indirect effects in community ecology: their definition, study and importance, *Trends Ecol. Evol.*, **6** (1991), 206–210. https://doi.org/10.1016/0169-5347(91)90023-Q
13. A. Kessler, R. Halitschke, K. Poveda, Herbivory-mediated pollinator limitation: negative impacts of induced volatiles on plant–pollinator interactions, *Ecology*, **92** (2011), 1769–1780. https://doi.org/10.1890/10-1945.1

14. D. Lucas-Barbosa, J. J. A. van Loon, M. Dicke, The effects of herbivore-induced plant volatiles on interactions between plants and flower-visiting insects, *Phytochemistry*, **72** (2011), 1647–1654. https://doi.org/10.1016/j.phytochem.2011.03.013

15. J. K. Conner, S. Rush, Effects of flower size and number on pollinator visitation to wild radish, *Raphanus raphanistrum*, *Oecologia*, **105** (1996), 509–516. https://doi.org/10.1007/BF00330014

16. E. L. Berlow, Strong effects of weak interactions in ecological communities, *Nature*, **398** (1999), 330–334. https://doi.org/10.1038/18672

17. M. Liu, K. Wang, Stochastic Lotka–Volterra systems with Lévy noise, *J. Math. Anal. Appl.*, **410** (2014), 750–763. https://doi.org/10.1016/j.jmaa.2013.07.078

18. H. Molla, S. Sarwardi, M. Sajid, Predator-prey dynamics with Allee effect on predator species subject to intra-specific competition and nonlinear prey refuge, *J. Math. Comput. Sci.*, **25** (2021), 150–165. https://doi.org/10.22436/jmcs.025.02.04

19. W. J. Li, W. R. Zhao, J. D. Cao, L. H. Huang, Dynamics of a linear source epidemic system with diffusion and media impact, *Z. Angew. Math. Phys.*, **75** (2024), 144. https://doi.org/10.1007/s00033-024-02271-2

20. B. A. Menge, Indirect effects in marine rocky intertidal interaction webs: patterns and importance, *Ecol. Monogr.*, **65** (1995), 21–74. https://doi.org/10.2307/2937158

21. P. Panday, N. Pal, S. Samanta, J. Chattopadhyay, Stability and bifurcation analysis of a three-species food chain model with fear, *Int. J. Bifurcation Chaos*, **28** (2018), 1850009. https://doi.org/10.1142/S0218127418500098

22. T. P. Nguyen, T. D. Do, T. T. Nguyen, Dynamical analysis of a stage-structured food-chain model under fear effect and anti-predator behavior, *J. Appl. Math. Comput.*, **71** (2025), 5867–5890. https://doi.org/10.1007/s12190-025-02451-x

23. R. A. Dakhil, S. J. Majeed, Three-species Lotka-Volterra food chain model with fear effect and hunting cooperation, *UTJsci*, **18** (2023). https://doi.org/10.32792/utj.v18i1.328

24. W. Li, L. Wang, Stability and bifurcation of a delayed three-level food chain model with Beddington–DeAngelis functional response, *Nonlinear Anal. Real World Appl.*, **10** (2009), 2471–2477. https://doi.org/10.1016/j.nonrwa.2008.05.004

25. M. S. W. Sunaryo, M. Mamat, Z. Salleh, Numerical simulation dynamical model of three species food chain with Holling type-II functional response, *Malays. J. Math. Sci.*, **5** (2011), 1–12.

26. S. Pal, S. Majhi, S. Mandal, N. Pal, Role of fear in a predator–prey model with Beddington–DeAngelis functional response, *Z. Naturforsch. A*, **74** (2019), 581–595. https://doi.org/10.1515/zna-2018-0449

27. I. Kollberg, H. Bylund, O. Huitu, C. Björkman, Regulation of forest defoliating insects through small mammal predation: reconsidering the mechanisms, *Oecologia*, **176** (2014), 975–983. https://doi.org/10.1007/s00442-014-3080-x

28. Y. Pei, G. Zeng, L. Chen, Species extinction and permanence in a prey–predator model with two-type functional responses and impulsive biological control, *Nonlinear Dyn.*, **52** (2008), 71–81. https://doi.org/10.1007/s11071-007-9258-6

29. J. R. Beddington, Mutual interference between parasites or predators and its effect on searching efficiency, *J. Anim. Ecol.*, **44** (1975), 331–340. https://doi.org/10.2307/3866
30. D. L. DeAngelis, R. A. Goldstein, R. V. O'Neill, A model for trophic interaction, *Ecology*, **56** (1975), 881–892. https://doi.org/10.2307/1936298
31. M. L. Rosenzweig, Paradox of enrichment: destabilization of exploitation systems in ecological time, *Science*, **171** (1971), 385–387. https://doi.org/10.1126/science.171.3969.385
32. F. Capone, On the dynamics of predator-prey models with the Beddington–De Angelis functional response, under Robin boundary conditions, *Ric. Mat.*, **57** (2008), 137–157. https://doi.org/10.1007/s11587-008-0026-9
33. V. T. Ta, A. Yagi, Dynamics of a stochastic predator-prey model with the Beddington-DeAngelis functional response, *Commun. Stoch. Anal.*, **5** (2011), 8. https://doi.org/10.31390/cosa.5.2.08
34. R. S. Cantrell, C. Cosner, On the dynamics of predator–prey models with the Beddington–DeAngelis functional response, *J. Math. Anal. Appl.*, **257** (2001), 206–222. https://doi.org/10.1006/jmaa.2000.7343
35. R. L. Song, *A Dynamical Study of the Plant-Pollinator-Herbivore System*, Ph.D. thesis, Northeast Normal University, 2023.
36. D. Gravel, F. Massol, M. A. Leibold, Stability and complexity in model meta-ecosystems, *Nat. Commun.*, **7** (2016), 12457. https://doi.org/10.1038/ncomms12457
37. B. Yang, Y. Cai, K. Wang, W. Wang, Optimal harvesting policy of logistic population model in a randomly fluctuating environment, *Physica A*, **526** (2019), 120817. https://doi.org/10.1016/j.physa.2019.04.053
38. Q. Liu, D. Jiang, Analysis of a stochastic within-host model of dengue infection with immune response and Ornstein-Uhlenbeck process, *J. Nonlinear Sci.*, **34** (2024), 28. https://doi.org/10.1007/s00332-023-10004-4
39. B. B. Zhang, H. Y. Wang, G. Y. Lv, Exponential extinction of a stochastic predator–prey model with Allee effect, *Physica A*, **507** (2018), 192–204. https://doi.org/10.1016/j.physa.2018.05.073
40. X. H. Wang, X. Y. Wang, W. L. Yang, Long time behavior of a rumor model with Ornstein-Uhlenbeck process, *Q. Appl. Math.*, **83** (2025), 437–454. https://doi.org/10.1090/qam/1701
41. S. J. Deng, W. J. Jiang, Levy process-driven mean-reverting electricity price model: the marginal distribution analysis, *Decis. Support Syst.*, **40** (2005), 483–494. https://doi.org/10.1016/j.dss.2004.05.010
42. X. Mao, *Stochastic Differential Equations and Applications*, 2nd edition, Woodhead Publishing, Oxford, 2008.
43. R. Khasminskii, *Stochastic Stability of Differential Equations*, Springer, Berlin, Heidelberg, 2012. https://doi.org/10.1007/978-3-642-23280-0
44. R. S. Lipster, A strong law of large numbers for local martingales, *Stochastics*, **3** (1980), 217–228. https://doi.org/10.1080/17442508008833146
45. Q. Luo, X. Mao, Stochastic population dynamics under regime switching, *J. Math. Anal. Appl.*, **334** (2007), 69–84. https://doi.org/10.1016/j.jmaa.2006.12.032

46. D. J. Higham, An algorithmic introduction to numerical simulation of stochastic differential equations, *SIAM Rev.*, **43** (2001), 525–546. https://doi.org/10.1137/S0036144500378302

47. S. E. Jørgensen, *Handbook of Environmental Data and Ecological Parameters: Environmental Sciences and Applications*, Pergamon Press, Oxford, 1979. https://doi.org/10.1016/C2013-0-05856-2

AIMS Press